Eur. Phys. J. B **32**, 35–42 (2003)
DOI: 10.1140/epjb/e2003-00071-1

THE EUROPEAN PHYSICAL JOURNAL B

Magnetic phases in $Mn_{1-x}Fe_xWO_4$ studied by neutron powder diffraction

E. García-Matres[1,a], N. Stüßer[1], M. Hofmann[1,b], and M. Reehuis[2]

[1] Hahn-Meitner Institut, Abteilung SF3, Glienicker Strasse 100, 14109 Berlin, Germany
[2] Institut für Physik, EKM, Universität Augsburg, 86159 Augsburg, Germany

Received 9 October 2002
Published online 14 March 2003 –

Abstract. The magnetic structures of $Mn_{1-x}Fe_xWO_4$ with $x = 0.0$, 0.16, 0.21, 0.225, 0.232, 0.24, 0.27, 0.29, and 1.0 were refined from neutron powder diffraction data. The magnetic phase diagram could be completed in the coexistence range of different magnetic structures up to $x = 0.29$. For the magnetic state at 1.5 K a commensurate antiferromagnetic structure with a propagation vector $\mathbf{k} = (\pm 1/4, 1/2, 1/2)$ was found for $x \leq 0.22$ while the magnetic spins order with $\mathbf{k} = (1/2, 0, 0)$ for $x \geq 0.22$. In the latter phase, additionally, weak magnetic reflections indexed to an incommensurate ordering with $\mathbf{k} = (-0.214, 1/2, 0.457)$ occur in the diffraction pattern up to $x = 0.29$ indicating the occurence of a reentrant phase. For $0.12 \leq x \leq 0.29$ the low temperature phases are separated from a magnetic high temperature phase showing only magnetic reflections indexed to a spin arrangement with $\mathbf{k} = (1/2, 0, 0)$. The magnetic phase diagram is discussed qualitatively considering random superexchange between the statistically distributed Mn^{2+}- and Fe^{2+}-ions in the coexistence range $0.12 \leq x \leq 0.29$ of different magnetic structures related to those of pure $MnWO_4$ and $FeWO_4$.

PACS. 75.30.Kz Magnetic phase boundaries (including magnetic transitions, metamagnetism, etc.) – 61.12.Ld Neutron diffraction

1 Introduction

Magnetic systems provide many nice possibilities to study the effects of disorder and frustration in condensed matter physics. A few years ago $MnWO_4$ has attracted interest since it could be a model system for an ANNNI model [1]. In the latter model frustration arises from the competition between a nearest neighbour ferromagnetic and a next nearest neighbour antiferromagnetic coupling in an uniaxial system [2]. Recently, we have reported that a mixed crystal of composition $Mn_{0.88}Fe_{0.12}WO_4$ shows simultaneously different types of long range magnetic order [3]. The observed spin arrangements are related to the magnetic structures of the pure compounds $MnWO_4$ and $FeWO_4$. A coexistence of two phases in different volume elements could be ruled out and we found strong evidence that the two different structures are formed on the same lattice: one structure is embedded as a cluster within the second structure. This unusual behaviour of two interpenetrating magnetic structures becomes possible by the various superexchange couplings between adjacent Mn–Mn, Fe–Fe, and Mn–Fe-ions *via* one or two intervening oxygen ions. For the $Mn_{0.88}Fe_{0.12}WO_4$ compound the $MnWO_4$-type magnetic structures were found to be the dominating ones and $FeWO_4$-type spin ordering is realized on a randomly diluted lattice only. This complex behaviour makes it tempting to establish the (x, T)-magnetic phase diagram for $Mn_{1-x}Fe_xWO_4$ in the interesting region of coexisting magnetic phases. The best suited technique to study the spatial correlations of the moments in the different phases is neutron diffraction. Single crystal studies like for $Mn_{0.88}Fe_{0.12}WO_4$ [3] were not possible due to the lack of suitable crystals with sufficient size and quality for single crystal neutron diffraction. Neutron powder diffraction was therefore applied in our studies.

Now we introduce shortly the crystal and magnetic structure of $MnWO_4$ and $FeWO_4$. Pure $MnWO_4$ and $FeWO_4$ are isomorphous and crystallize in the monoclinic space group is P2/c [1,4,5]. The transition metal and the tungsten are surrounded by distorted oxygen octahedra and form alternating layers in the *bc*-plane (Fig. 1).

The antiferromagnetic structures of $MnWO_4$ and $FeWO_4$ are well known and a group theoretical analysis of possible spin arrangements is given in the literature [1,4]. The compound $MnWO_4$ forms two incommensurate collinear magnetic structures, one between 13.5 K and 12.3 K denoted as AF3, and another between 12.3 K and 8.0 K called AF2. Both structures have the same propagation vector $\mathbf{k} = (-0.214, 1/2, 0.457)$, but they

[a] e-mail: garcia-matres@hmi.de
[b] *Present address:* FRM-II, Technische Universität München, 85747 Garching, Germany

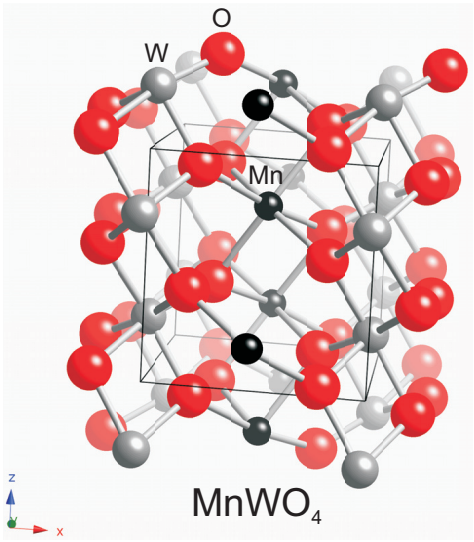

Fig. 1. Crystal structure (SPG: P2/c) of (Mn,Fe)WO_4. The $(Mn/Fe)^{2+}$-ions and the W^{6+}-ions are surrounded by distorted oxygen octahedra. Frame indicates unit cell.

differ with respect to the orientation of the moments. In the magnetic ground state AF1 below 8 K the propagation vector is commensurate with $\mathbf{k} = (\pm 1/4, 1/2, 1/2)$ (Fig. 2a). The collinear antiferromagnetic spin arrangement in $FeWO_4$ below $T_N = 76$ K with $\mathbf{k} = (1/2, 0, 0)$ will be denoted as AF4 (Fig. 2b). The spins are confined to the *ac*-plane for the phases AF1, AF3, and AF4. An additional component of the moment along the [0 1 0] direction occurs in phase AF2.

2 Experimental procedures

The specimens were prepared by solid state reaction: appropriate portions of $MnWO_4$ and $FeWO_4$ were mixed and preheated at 1000 °C for 6 hours. Then the preheated sample was ground and heated again to 1000 °C for one week. The quality of some specimens was tested and determined to be of single phase using neutron powder diffraction at the high resolution instrument E9 at the BERII reactor of the Hahn-Meitner-Institut. Experiments were done using a neutron wavelength of 1.798 Å provided by a 5 1 1 Ge-monochromator and chosing a 18′–20′ collimation setup for α_1 as inpile and α_2 in front of the sample. The detector bank consists of 64 × 10′-collimations in front of 64 ^{3}He-single detector tubes.

The magnetic diffraction patterns were collected mainly at the diffractometer E6. This instrument is equipped with a double focusing 0 0 2 pyrolythic graphite monochromator providing a wavelength of 2.4 Å. Second order contamination is suppressed below 10^{-3} by a pyrolythic graphite filter. Scattered neutrons are detected by a linear position sensitive BF_3 proportional counter with an angular resolution of 0.1°. Further details about the instruments E9 and E6 can be found in [6] and [7], respectively.

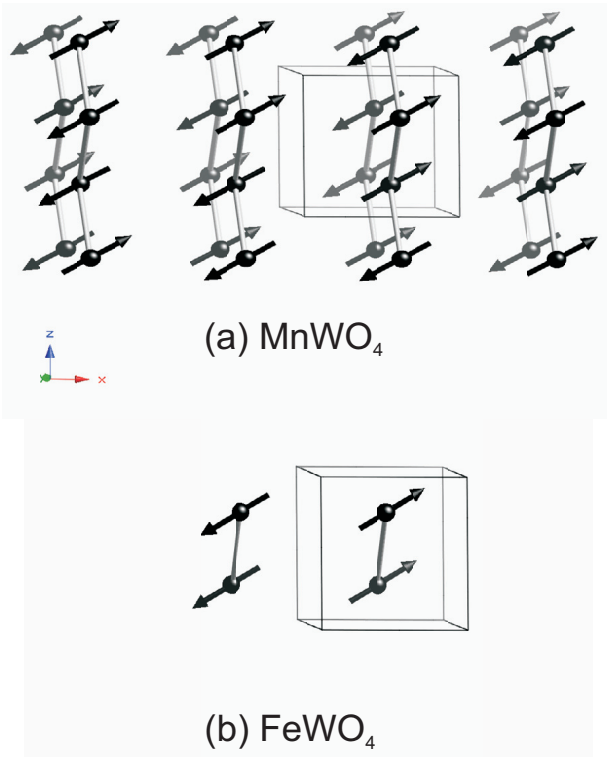

Fig. 2. Magnetic structure of the ground state for $MnWO_4$ (a) and $FeWO_4$ (b). Frames indicate the crystallographic unit cell.

3 Results of the refinements

Rietveld profile refinements for $Mn_{1-x}Fe_xWO_4$ powders with $x = 0.0$, 0.16, 0.21, 0.225, 0.232, 0.24, 0.27, 0.29, and 1.0 were carried out with the Fullprof program [8] using the coherent nuclear scattering lengths $b(\mathrm{Mn}) = -3.73$ fm, $b(\mathrm{Fe}) = 9.54$ fm, $b(\mathrm{W}) = 4.77$ fm, and $b(\mathrm{O}) = 5.803$ fm. The background was fitted to a polynomial function and the lineshape of peaks was considered as Gaussian for the data collected at E6 and as pseudo-Voigt convoluted with an axial divergence asymmetry function for the data collected at E9.

For all specimens the crystallographic structure can be well described within the monoclinic space group P2/c and the analysis indicates a statistical distribution of the Mn- and Fe-ions on the Wyckoff position 2*f*. The concentration of the Mn- and Fe-ions, obtained from refinements of data collected at E9, agrees well with the nominal concentration used as starting material for the sample preparation. The precision in the determination of the Fe/Mn occupation at the 2*f* site is high due to the high contrast in scattering lengths between Mn and Fe. A monotonous decrease of the monoclinic angle is found with increasing Fe-concentration, consistent with the difference in the monoclinic angle of the pure phases $MnWO_4$ and $FeWO_4$ which are about 91.1° and 90°, respectively. The lattice constants determined for samples measured at E9 follow Vegard's law with a linear concentration dependence of the lattice constants *a*, *b*, and *c*. They are in reasonable agreement with values reported in [5]. In the following

Table 1. Results of the neutron powder studies of $Mn_{1-x}Fe_xWO_4$. Lattice parameters a, b, c, and β, as well as the parameter y for (Mn, Fe) position at $2f$ are listed. The experimental moments of the (Mn, Fe) and their angles φ, θ to the monoclinic a- and c-axis are given for each magnetic phase. Finally the size of the total mean moment is given per magnetic ion in μ_B. Numbers in parentheses are the standard deviations obtained from the least squares analyses.

$Mn_{1-x}Fe_xWO_4$	$x = 0.0$[a]	$x = 0.16$	$x = 0.21$[a]	$x = 0.225$	$x = 0.232$	$x = 0.24$	$x = 0.27$	$x = 0.29$	$x = 1.0$[a]
a (Å)	4.82340(7)	4.7806(6)	4.80125(5)	4.7766(5)	4.7841(6)	4.7747(7)	4.7927(6)	4.7747(6)	4.73022(6)
b (Å)	5.7529(1)	5.712(1)	5.74127(5)	5.7097(9)	5.7208(8)	5.7094(9)	5.7336(9)	5.7116(7)	5.70578(7)
c (Å)	4.99193(3)	4.9584(8)	4.98459(5)	4.9561(7)	4.9700(7)	4.9611(8)	4.9809(7)	4.9618(6)	4.95230(5)
β (degrees)	91.103(1)	90.86(1)	90.7901(8)	90.78(1)	90.756(9)	90.75(1)	90.72(1)	90.695(7)	89.7268(8)
y (Mn/Fe)	0.6865(8)	0.705(3)	0.692(2)	0.693(1)	0.6824(9)	0.682(1)	0.681(1)	0.6764(9)	0.6697(8)
M(AF1) (1/4,1/2,1/2)	4.29(5)	4.65(6)	4.52(4)	2.62(5)					
φ ($\theta = 90°$)	36(1)	23(1)	25(1)	30.2(4)					
M(AF4) (1/2,0,0)				2.96(3)	3.77(3)	3.92(5)	4.24(4)	4.49(5)	4.69(3)
φ ($\theta = 90°$)				30.3(4)	27.8(4)	29.1(5)	30.1(3)	30.1(4)	25.7(3)
M(AF2/AF3) (k_x,0,k_y)				2.16(5)	2.53(5)	2.29(7)	1.70(1)	1.29(7)	
φ				30.3(4)	29.0[b]	29.1(5)	30 (14)	36(9)	
θ				141(4)	170[b]	156(7)	139(9)	90.00	
$\sqrt{M_i^2}$				4.5(1)	4.54(8)	4.5(1)	4.57(5)	4.7(1)	

[a] Data from the diffractometer E9.
[b] Fixed parameters.

we present the results of the refinements of the magnetic structures. Specimens of different concentrations are grouped according to their similar magnetic behaviour.

3.1 Magnetic structure of $Mn_{1-x}Fe_xWO_4$ with x = 0.16, 0.21

Below their Néel temperature all specimens with $0.16 \leq x \leq 0.21$ order first antiferromagnetically in a structure with a propagation vector $\mathbf{k} = (1/2, 0, 0)$. This magnetic structure agrees well with the spin arrangement AF4 as present in $FeWO_4$ with the spins lying inside the ac-plane and inclined by an angle of about 28° with respect to the a-axis. At a lower temperature T^{II} these specimens show a magnetic phase transition to the commensurate AF1 structure with $\mathbf{k} = (\pm 1/4,\ 1/2,\ 1/2)$. The moments are again collinearly aligned inside the ac-plane inclined by about the same angle to the a-axis as present in the high temperature phase AF4. No indication was found for an incommensurate spin structure with a propagation vector $(k_x, 1/2, k_z)$ as has been found for powder specimens of mixed crystals with $x \leq 0.12$. As an example observed and calculated pattern of $Mn_{0.79}Fe_{0.21}WO_4$ collected at 12 K and 2 K are shown in Figure 3. Consistent with analyses on $MnWO_4$ [1] the best fit to the data uses a model in which the magnetic moments have no component along [0 1 0]. Results of the refinements are quoted in Table 1.

A study of the temperature dependence of the crystal and magnetic structure has been carried out for the $Mn_{0.79}Fe_{0.21}WO_4$ sample between 1.5 K and 40 K using high resolution data sets collected at E9. In the magnetically ordered state simultaneous refinements of the nuclear and the antiferromagnetic structure were performed with a total of 25 variable parameters: the zero point, the scale factor, six parameters for background fitting, three profile parameters, four lattice parameters, eight positional parameters, the moment size and its direction in the ac-plane. In the fits of data sets collected below T_N the occupancies and the isotropic temperature factors were fixed to values obtained from a refinement of the crystal structure using data collected at 25 K with the sample in the paramagnetic state. The temperature dependence of the lattice constants is shown in Figure 4. Remarkable are the sudden decrease in the lattice constant b, and an increase in the lattice constants a and c across the magnetic phase transition from phase AF1 to AF2. Below 8 K, all lattice and positional parameters are nearly temperature independent. Beside changes in the lattice constants we observe a shift in the parameter y of the Mn/Fe position (1/2 y 1/4) in phase AF4 between 10 K and 20 K (Fig. 4). All the other positional parameters for the W- and O-ions did not change significantly within the experimental error. Measurements to study possible magnetoelastic effects in $MnWO_4$ and $FeWO_4$ have been started for comparison. An increase of b at the magnetic transition from phase AF4 to phase AF1 seems to be present, however, has to be put on a firmer basis.

The temperature behaviour of the mean magnetic moment M for the $Mn_{0.79}Fe_{0.21}WO_4$ compound was obtained by using $M \sim cI^{1/2}$ with I the integrated intensities of the Bragg reflections 1/4 1/2 1/2 and 1/2 0 0 for the two structures AF1 and AF4, respectively (Fig. 5c). The constant c was determined using the moment obtained from a simultaneous refinement of the nuclear and magnetic structure at one temperature. The mean moment determined in this way represents a moment size averaged over the whole sublattice of Mn/Fe-positions. In case

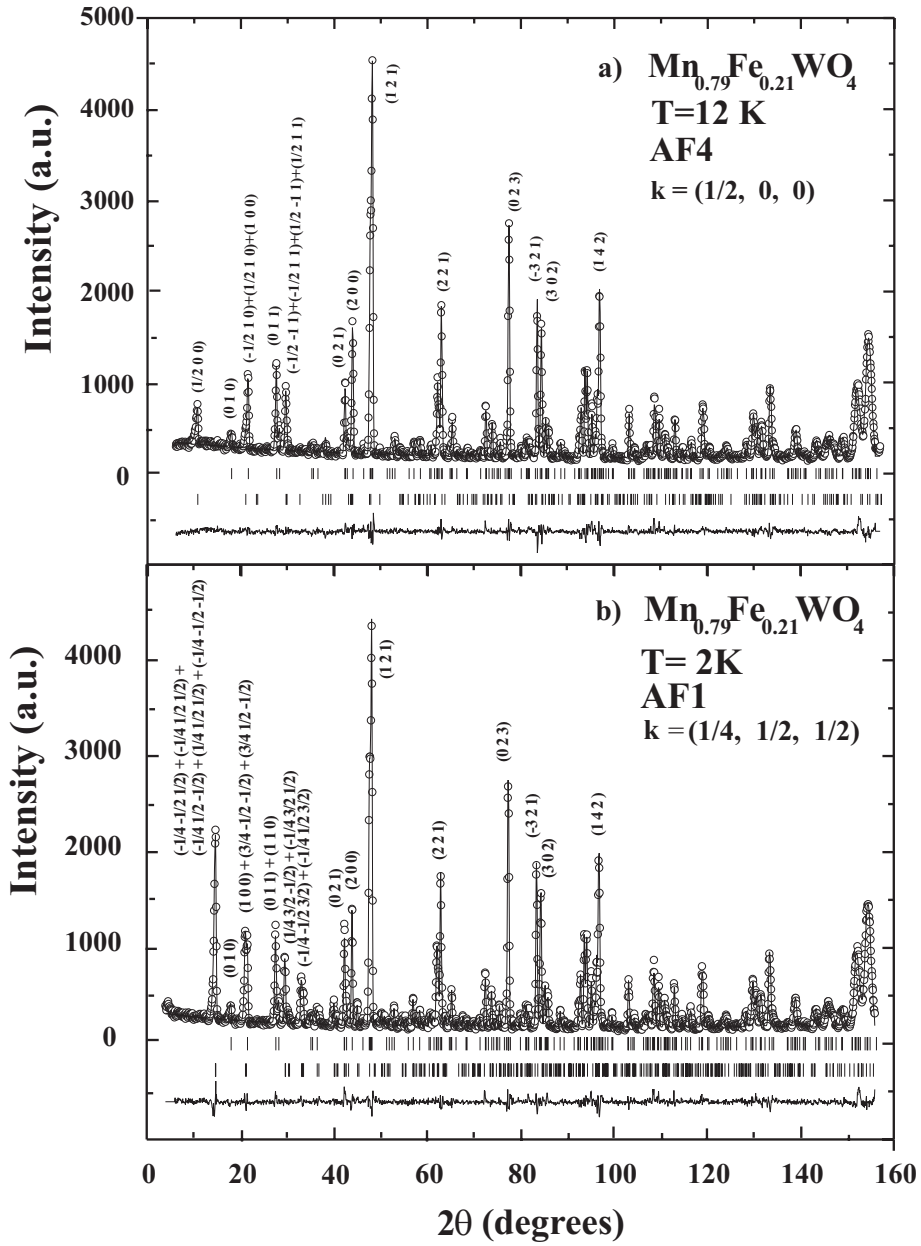

Fig. 3. Neutron powder diffractograms with fit and difference pattern of $Mn_{0.79}Fe_{0.21}WO_4$ at 12 K (a) and 2 K (b). Upper and lower row of bars in the lower part of the figures mark positions of nuclear and magnetic reflections, respectively. Few magnetic and nuclear reflections are labelled by their Miller indices (hkl).

the ordered moments are limited to a smaller number of positions on this sublattice the size of the local moment will be larger. Comments on this are given in the discussion below. Data used for the analysis were measured at the instrument E6 in order to have $M(T)$ at a sufficient number of different temperatures. For phase AF1 we observe a gradual decrease in M with rising temperature. At $T^{II} \sim 7.5$ K, the transition point to phase AF4, the moment suddenly reduces by about 25%. Then M continues to decrease gradually until it vanishes at $TN \approx 24$ K in a manner typical for a second order phase transition. Important crystallographic and magnetic parameters for different magnetic phases AF1 and AF4 of the investigated specimens are listed in Table 1.

3.2 Magnetic structure of $Mn_{1-x}Fe_xWO_4$ with $x = 0.232, 0.24, 0.27, 0.29$

At T_N the paramagnetism changes to an ordering with an AF4-type magnetic structure. Below the transition temperature T^{III} additional magnetic Bragg reflections occur which can be indexed to an incommensurate structure

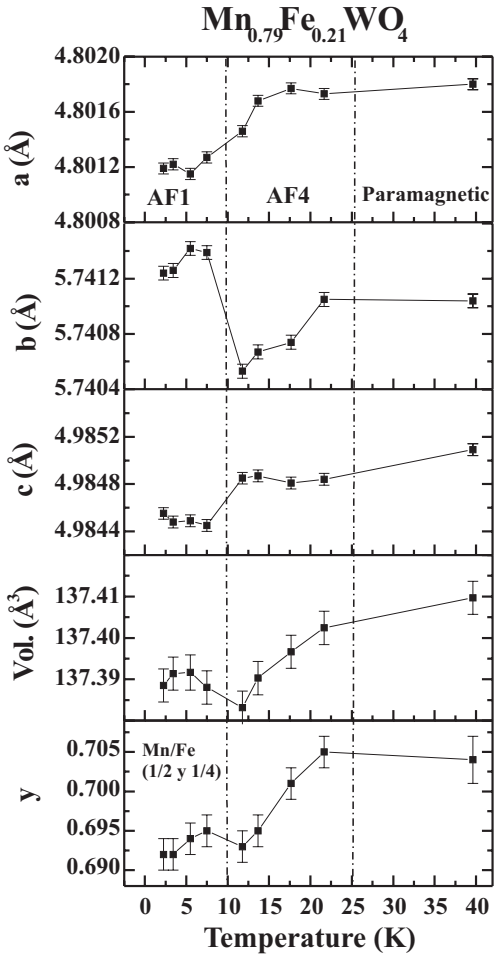

Fig. 4. Temperature behaviour of the lattice constants a, b, c, the unit cell volume V, and the positional parameter y of the Mn/Fe-ion for $Mn_{0.79}Fe_{0.21}WO_4$.

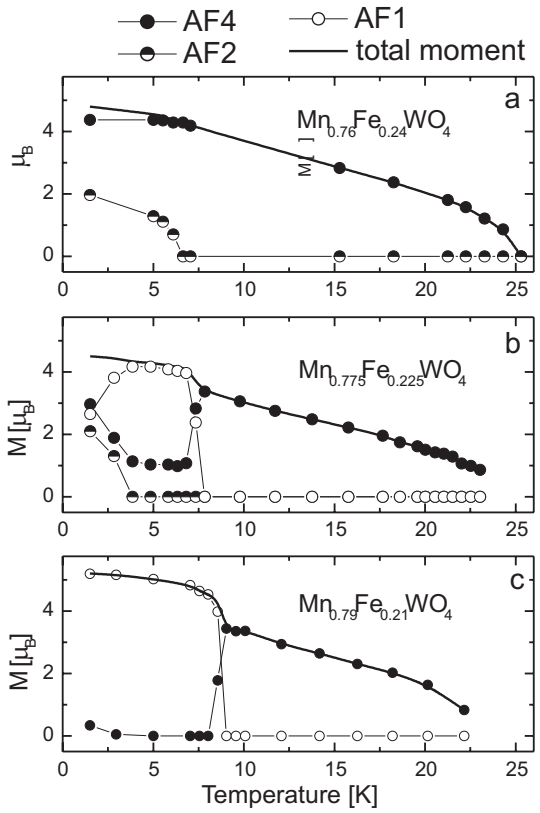

Fig. 5. Temperature behaviour of the mean magnetic moment for the observed magnetic structures of $Mn_{0.76}Fe_{0.24}WO_4$ (a), $Mn_{0.775}Fe_{0.225}WO_4$ (b), and $Mn_{0.79}Fe_{0.21}WO_4$ (c). Solid line is the total mean moment per site calculated from $M = (\Sigma M_i^2)^{1/2}$ where i refers the different structures present.

with $\mathbf{k} = (-0.21, 1/2, 0.457)$. A model of a sinusoidal modulated spin arrangement reproduces these reflections very well. This spin arrangement is very similar to the structure AF2 found in the temperature region between 12.3 K and 8 K for $MnWO_4$ [1]. In particular, the moments have now an additional component along the [0, 1, 0] direction. Important magnetic parameters are given in Table 1.

A diffraction pattern of $Mn_{0.76}Fe_{0.24}WO_4$ collected at 1.5 K is shown in Figure 6. The temperature behaviour of the ordered magnetic moment for the observed structures AF4 and AF2 as obtained from the temperature dependence of the 1/2 0 0 and 0.21 1/2 0.54 reflections, respectively, is displayed in Figure 5a. Below $T^{III} \approx 7$ K the mean moment for structure AF4 is already close to saturation while a mean ordered moment for structure AF2 occurs and increases towards lower temperature.

3.3 Magnetic structure of $Mn_{1-x}Fe_xWO_4$ with x = 0.225

$Mn_{0.775}Fe_{0.225}WO_4$ has a concentration x which is just located between the two concentration regions of specimens discussed in sections a) and b) above. Diffraction patterns at different temperatures collected at the instrument E6 are shown in Figure 7. First a magnetic ordering occurs below $T_N = 23$ K to structure AF4. At a lower temperature $T^{II} \approx 7.5$ K the intensity of reflections related to structure AF4 are reduced significantly and nearly vanish in the temperature region between 7 K and 3 K. Instead a new structure of the AF1 type is showing up. Below $T^{IV} \approx 3$ K the Bragg reflections related to AF1 decrease in intensity while reflections belonging to structure AF4 increase their intensity again. Moreover, we now observe tiny reflections related to an IC structure AF2. The mean magnetic moments for the various structures determined from the temperature dependence of the different reflections and calibrated using the result of refinements of diffraction patterns measured at selected temperatures are shown in Figure 5b. Magnetic and crystallographic parameters are listed in Table 1.

4 Discussion and conclusions

The experimental results from this work together with a few results from former investigations [1,3] allow now to present the (x, T) magnetic phase diagram for

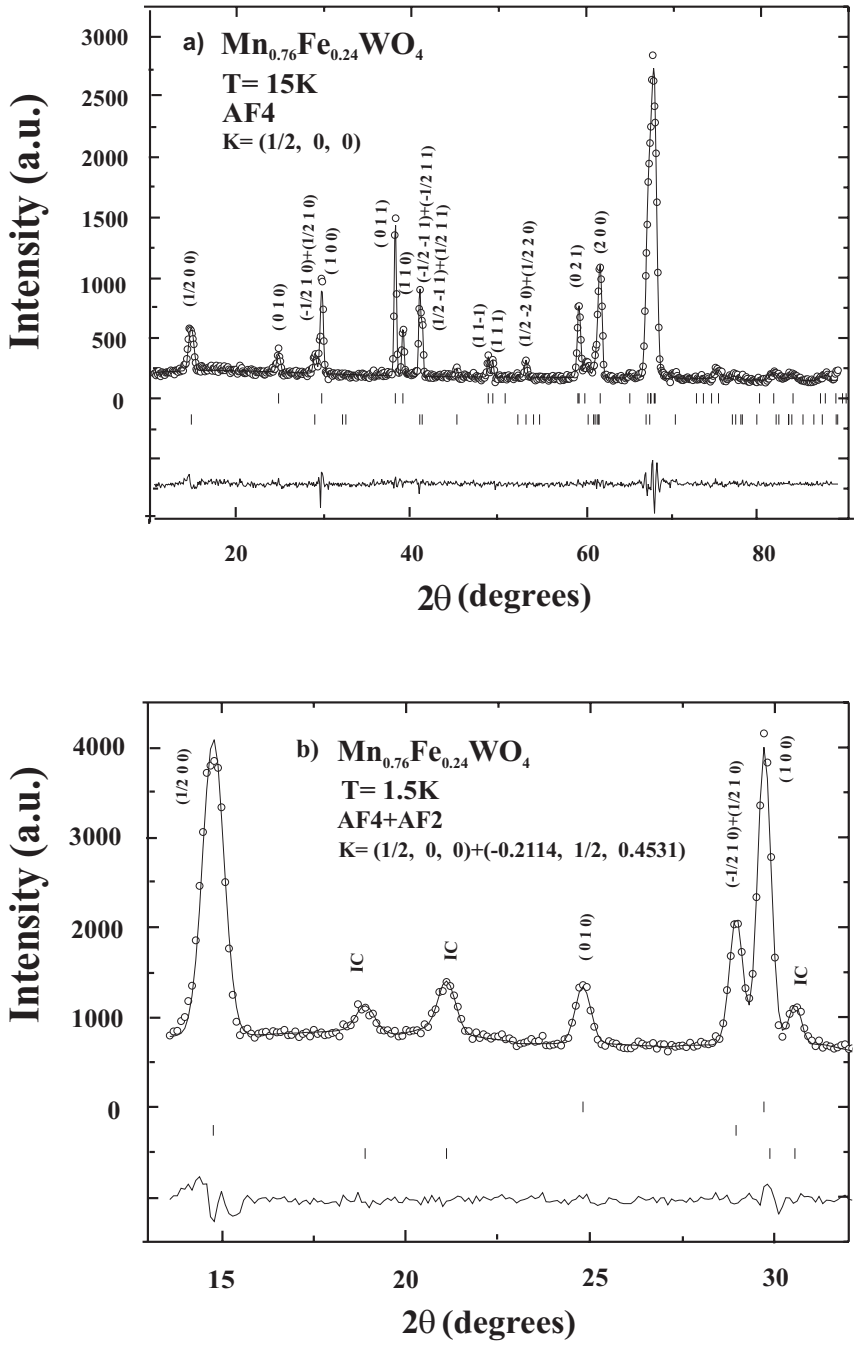

Fig. 6. Neutron powder diffractogram with fit and difference pattern of $Mn_{0.76}Fe_{0.24}WO_4$ at 15 K (a) and 1.5 K (b). Upper and lower row of bars in the lower part of the figures mark positions of nuclear and magnetic reflections, respectively. Few magnetic and nuclear reflections are labelled by their Miller indices (*hkl*). IC in part (b) indicates reflections for incommensurate structure.

$Mn_{1-x}Fe_xWO_4$ with $0 \leq x \leq 0.29$ as shown in Figure 8. The extraordinary rich phase diagram with regions of coexistence of different phases is related to the presence of superexchanges *via* one or two intervening oxygen ions along different paths between Mn–Mn, Fe–Fe, or Mn–Fe pairs of neighbours [9–12]. The participating magnetic ions Mn or Fe and the exchange path under consideration determine the sign and magnitude of the interaction. Therefore, the presence of randomly distributed Fe-ions on the Mn-ion positions introduce some random exchange [13]. One expects a change in the mean exchange coupling and a corresponding change in the critical temperature for low concentrations of substituted ions. A breakdown of long range order for the structure considered should occur at critical percolation threshold. Beside the random exchange one has to consider a differing

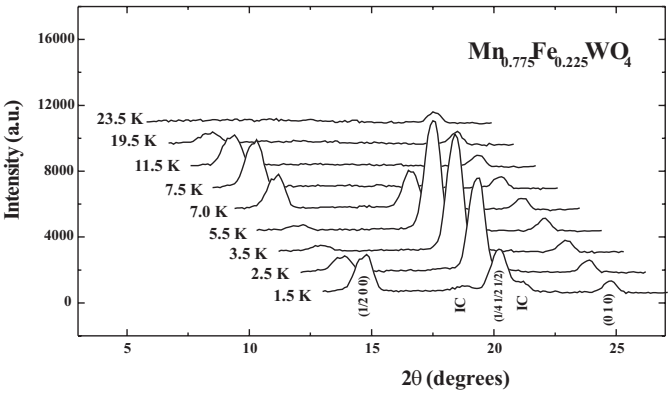

Fig. 7. Neutron powder diffractogram at different temperatures for $Mn_{0.775}Fe_{0.225}WO_4$.

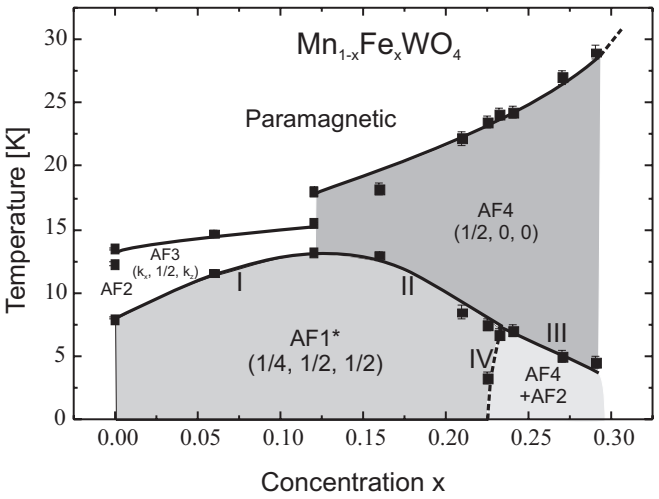

Fig. 8. Magnetic (x, T) phase diagram of $Mn_{1-x}Fe_xWO_4$. Phases are labelled by using AF1, AF2, AF3, and AF4 for the observed spin arrangements. Phase boundaries are denoted by I, II, III and IV. Lines are guide for the eyes. *Reflections (1/2 0 0) and (5/2 0 0) of a magnetic phase observed in a $Mn_{0.88}Fe_{0.12}WO_4$ single crystal below 13 K were not accessible in the powder experiments due to the low intensity.

anisotropy as well: the Mn-moments in all collinear $MnWO_4$ structures have a different orientation in the *ac*-plane than the Fe-moments in $FeWO_4$. All $Mn_{1-x}Fe_xWO_4$ crystals studied, however, show that the moments of Mn and Fe in most cases take on nearly the orientation as observed for $FeWO_4$. This demonstrates a dominating anisotropy for the Fe^{2+}-moments compared to the Mn^{2+}-moment which originates from a half filled *d*-shell with no orbital moment.

Now we will qualitatively consider the random exchange behaviour for the complex system $Mn_{1-x}Fe_xWO_4$. The high Néel temperature of 76 K for $FeWO_4$ compared to 13.5 K for $MnWO_4$ indicates an effectively stronger coupling between the Fe-ions to form an AF4 structure as is present between the Mn-ions to form the structures AF1, AF2, and AF3. A small substitution up to 12% of Mn-ions by Fe-ions leads to a stabilization of $MnWO_4$-type structures. It is obvious from the magnetic phase diagram (Fig. 8) that the Néel temperature increases from 13.5 K to 15.5 K and the IC-C transition to phase AF1 increases from 8 K to 12 K in going from $MnWO_4$ to $Mn_{0.88}Fe_{0.12}WO_4$. Moreover, the propagation vector for the IC-phase(s) changes from (−0.214, 0.5, 0.457) to (−0.235, 0.5, 0.49). The latter value approaches the propagation vector (1/4, 1/2, 1/2) of the commensurate structure AF1. Beyond a concentration of 12% Fe the incommensurate $MnWO_4$-type phases are only stable in a very narrow temperature region and they could not be observed in our powder measurements with a Fe concentration of 16% Fe and above. Now long range magnetic order sets in below T_N with structure AF4 typical for $FeWO_4$. It has to be noted that we already observed the structure AF4 in our former experiments at a single crystal of $Mn_{0.88}Fe_{0.12}MnWO_4$ [3]. A small broadening of the peaks and the gradual increase in intensity with decreasing temperature point to short range order though with a large correlation length. As suggested earlier it becomes possible that two different structures are present on the same sublattice. One has to imagine one phase realized on a part of the lattice points which is interpenetrated by a second phase percolating on other lattice points [3,14].

In the concentration range $0.12 < x \leq 0.21$ the samples mainly order at T_N in a high temperature phase AF4 separated from a low temperature phase AF1 at T_c. Now T_N increases stronger with growing Fe-concentration, and from $x = 0.12$ up to $x = 0.21$ the temperature T_c for the transition to the commensurate structure AF1 decreases, *i.e.* $MnWO_4$-type structures are destabilized. Above an Fe concentration of 23% structure AF1 is not formed any more and structure AF4 is the dominating one at all temperatures below T_N. Surprising is the additional occurrence of tiny reflections which can be attributed again to the presence of an incommensurate structure similar to AF2 found in $MnWO_4$ in the temperature range between 13.5 K and 8 K. This is an astonishing reminiscence of the magnetic behaviour of $MnWO_4$ where the incommensurate structure AF2 is observed as a high temperature phase as is usual. Now the IC structure is observed at low temperatures. Moreover, the propagation vector is very close to the value for $MnWO_4$, which surprises again since the replacement of Mn by Fe first leads to a shift of the propagation vector towards (1/4, 1/2, 1/2) at values $x \leq 0.12 - 0.16$. One should, however, keep in mind that the IC structure seen for Fe concentrations between 23% and 29% is probably percolating on a very diluted lattice interpenetrating the dominant $FeWO_4$-type spin ordering AF4.

The specimen with $x = 0.225$ shows a magnetic behaviour which shares in common the behaviour of the specimens having a lower and a higher concentration in x. It first orders in structure AF4 below $T_N \approx 23$. Below the temperature $T^{II} \approx 7.5$ K one observes a change to structure AF1 known from samples with $x \leq 0.21$. Another

change in the magnetic structure occurs at $T^{IV} \approx 3$ K: the presence of structure AF1 decreases and one observes structure AF4 together with a structure AF2 towards lower temperature similar to the behaviour known from samples with $0.23 \leq x \leq 0.29$. One can rule out to attribute this behaviour to fluctuations in the order of $\Delta x \approx 0.02$ for the concentration x. If such a concentration gradient would be present one could not explain the vanishing of the intensities related to structure AF4 around T^{II}. Our measurements indicate that the phase boundary IV separating specimens described in Sections 3.1 and 3.2 (see above) is bended towards higher concentration with increasing temperature (see Fig. 8). Then $Mn_{0.775}Fe_{0.225}WO_4$ first enters phase AF1 at an intermediate temperature T^{II}. Towards lower temperature one approaches (or crosses) the phase boundary IV. Our diffraction data collected at the lowest temperature of 1.5 K do not allow to decide whether the simultaneous observations of phases AF1 and AF4 together with AF2 results from the presence of a mixed phase or is related to the forming of domains due to the presence of small gradients $\Delta x < 0.02$. Both spin arrangements give the same diffraction pattern. The temperature behaviour of the mean moments between 3 K and 1.5 K (Fig. 5b), however, points to a ground state similar to the one observed for specimens with $0.23 \leq x \leq 0.29$.

In all magnetic phase transitions we observe a sudden increase of the mean magnetic moment towards lower temperatures (Figs. 5a–c). For our complex random exchange system this probably indicates the incorporation of additional spins in the ordered state not yet ordered in the high temperature phase. This ordering of additional spins corresponds to a gain in the overall energy at the expense of some entropy.

Our measurements at the $Mn_{0.79}Fe_{0.21}WO_4$ show a significant change in the lattice constants, an increase in b accompanied by some decrease in a and c, at the transition from structure AF4 to AF1. This magnetoelastic behaviour, which corresponds mainly to a shape magnetostriction, was not seen so clearly in the specimens with different concentrations. This can be understood since the ordered moment is largest at the transition for the specimen with 21% Fe. It may be interesting to note that both structures are collinear with the same direction for the magnetic anisotropy. Further studies are planned in the future.

In conclusion mixed crystals $Mn_{1-x}Fe_xWO_4$ in the concentration range $0 \leq x \leq 0.29$ show a very complex and rich magnetic (x, T) phase diagram which is governed by the competition of various superexchange couplings. A detailed quantitative understanding of the different phases is hampered by a detailed knowledge of the individual exchange paths between the magnetic transition metals. Despite that a qualitative understanding of the dominating phases seems to be intuitive considering the magnetic phases of the pure end members $MnWO_4$ and $FeWO_4$, and in particular, taking into account there different strengths in the average exchange coupling reflected in their Néel temperatures with $T_N = 13.5$ K and 76 K, respectively. Then the presence of random exchange can account for some main features of the phase diagram. $MnWO_4$ type structures are only observed up to Fe concentrations of $x = 0.29$. The $FeWO_4$-type structure AF4 already forms as a high temperature phase for $x \geq 0.12$ due to the "stronger exchange of the Fe-ions". Mn-ions are incorporated to overcome the percolation threshold which is about $x = 0.25$ determined from studies at the system $Mg_{1-x}Fe_xWO_4$ [5]. At lower temperatures $MnWO_4$-type structures are still observed for $x < 0.225$. Now temperature is low enough so that an ordering becomes possible caused by the "weaker exchange of the Mn-ions". More Mn/Fe ions are ordered compared to the $FeWO_4$-type structure at higher temperature. Phase transitions are then governed by the detailed balance between energy and entropy. Regions of mixed phases occur for $0.12 \leq x \leq 0.29$. Finer details like our interesting observation of an incommensurate AF2 spin order at low temperature on a diluted sublattice for specimens with $0.22 \leq x \leq 0.29$ ask for theoretical model calculations to get more insight to the possible spin arrangements in a system as complex as $Mn_{1-x}Fe_xWO_4$.

We thank Mrs. Pfannenstiel and Mr. Rönnfeldt for the preparation of the powder specimens and Prof. D. Hohlwein for critical reading of the manuscript.

References

1. G. Lautenschläger, H. Weitzel, T. Vogt, R. Hock, A. Böhm, M. Bonnet, H. Fuess, Phys. Rev. B **48**, 6087 (1993), and references therein
2. W. Selke, *Phase Transitions and Critical Phenomena* Vol. 15, edited by C. Domb, J.L. Lebowitz (Academic Press, New York, 1992)
3. N. Stüßer, Y. Ding, M. Hofmann, M. Reehuis, B. Ouladdiaf, G. Ehlers, D. Günther, M. Meißner, M. Steiner, J. Phys. Cond. Matt. **13**, 2753 (2001)
4. D. Ülkü, Zeitschrift für Kristallographie **124**, 192 (1967)
5. H.A. Obermayer, H. Dachs, H. Schröcke, Solid State Commun. **12**, 779 (1973)
6. D.M. Többens, N. Stüßer, K. Knorr, H.M. Mayer, G. Lampert, Mat. Science Forum **378-381**, 288 (2001)
7. N. Stüßer, M. Hofmann, Nucl. Instr. Meth. Phys. Res. A **482**, 744 (2002)
8. J. Rodríguez-Carvajal, FullProf: A program for Rietveld refinement and Pattern Matching Analysis, *Abstract of the Sattelite Meeting on Powder Diffraction on the XV Congres of the IUCr, Toulouse, 127, 1990*
9. H. Ehrenberg, H. Weitzel, H. Fuess, B. Hennion, J. Phys. Cond. Matt. **11**, 2649 (1999)
10. H. Weitzel, H. Langhof, J. Magn. Magn. Mater. **4**, 265 (1977)
11. J.B. Goodenough, *Magnetism and Chemical Bond* (John Wiley, New York, 1963)
12. J. Kanamori, J. Phys. Chem. Solids **10**, 87 (1959)
13. D.S. Fisher, G.H. Grinstein, A. Khurana, Phys. Today **41**, 56 (1988)
14. F. Wegner, Solid State Commun. **12**, 785 (1973)